NATIONAL ADVISORY COMMITTEE FOR AERONAUTICS

TECHNICAL NOTE 3454

EFFECT OF A DISCONTINUITY ON TURBULENT BOUNDARY-LAYER-THICKNESS PARAMETERS WITH APPLICATION TO SHOCK-INDUCED SEPARATION

By Eli Reshotko and Maurice Tucker

Lewis Flight Propulsion Laboratory
Cleveland, Ohio

Washington
May 1955

ERRATA

NACA TN 3454

EFFECT OF A DISCONTINUITY ON TURBULENT BOUNDARY-LAYER-THICKNESS PARAMETERS WITH APPLICATION TO SHOCK-INDUCED SEPARATION

By Eli Reshotko and Maurice Tucker

May 1955

Page 4: The second and third paragraphs of the APPLICATIONS section should be replaced by the following paragraphs:

Reference 13 suggests that for turbulent boundary-layer separation H_i ranges from 1.8 to 2.6. With $H_{i,2} = 2.2$, the Mach number ratio M_2/M_1 obtained from equation (7) is 0.762. As shown in figure 3(a), this Mach number ratio yields pressure ratios from the oblique-shock relations that are in good agreement with "first peak" pressure ratios obtained on forward-facing steps in references 8 to 11. The data of reference 12 fall below the rest; however, figure 9 of this reference suggests that these data may have been taken in the transition region. A Mach number ratio of 0.81 yields pressure ratios in good agreement with "inflection-point" pressure ratios obtained on wedges (fig. 8 of ref. 8). According to reference 8, these first-peak- and inflection-point pressure ratios provide first approximations to the pressure ratios for which separation is likely to be encountered on control-surface configurations.

The separation pressure ratios obtained from the oblique-shock relations and equation (4) of reference 4 for a Mach number ratio of $\sqrt{0.494} = 0.703$ are presented in figure 3(b) as are also the pressure ratios obtained from equation (8) of reference 4. These pressure ratios are compared, as in reference 4, with the "inflection point" pressure ratios for wedges reported in reference 8. Inasmuch as the results from equations (4) and (8) of reference 4 should be in agreement, the discrepancy shown in figure 3(b) suggests that the oblique-shock linearization used in equation (8) of reference 4 is inadequate.

Page 12: The sentence following equation (C1) should read "Using relations (B4)" instead of "Using relations (B2)".

Page 20: Figure 3 should be replaced by the attached figure.

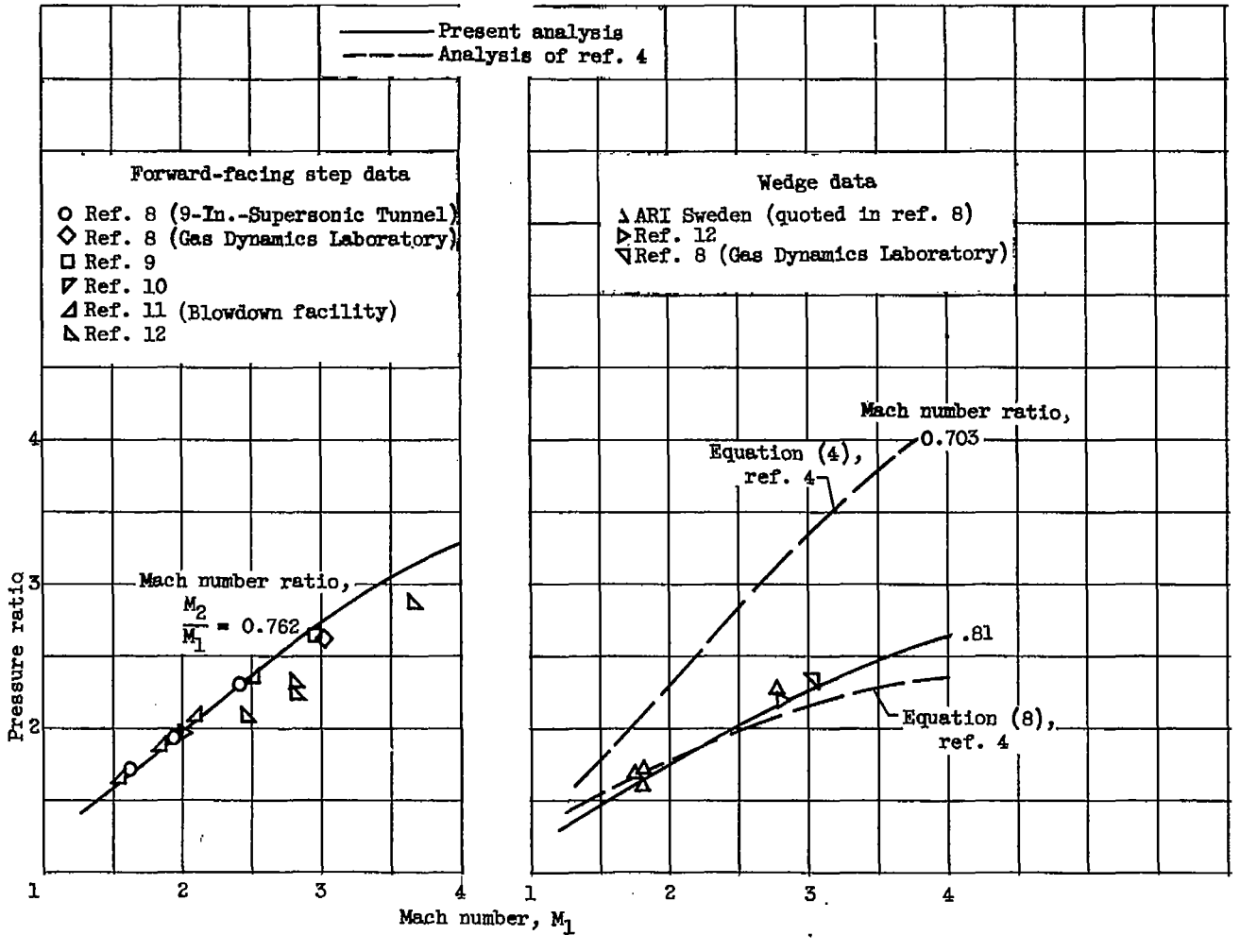

(a) First peak pressure ratio for forward-facing steps.

(b) Inflection-point pressure ratios obtained on wedges.

Figure 3. - Pressure ratios associated with shock-induced, turbulent, boundary-layer separation.

NATIONAL ADVISORY COMMITTEE FOR AERONAUTICS

TECHNICAL NOTE 3454

EFFECT OF A DISCONTINUITY ON TURBULENT BOUNDARY-LAYER-THICKNESS PARAMETERS WITH APPLICATION TO SHOCK-INDUCED SEPARATION

By Eli Reshotko and Maurice Tucker

SUMMARY

The problem of shock-induced turbulent boundary-layer separation was analyzed by an approximate method. This method is based on a moment-of-momentum equation and calculates the change of boundary-layer-thickness parameters and form factor caused by a discontinuity where the effects of friction can be neglected. The form of the result suggests that the Mach number ratio across the shock is a characteristic parameter for defining shock-induced separation. The method is also used to estimate the effects of mass transfer on the boundary-layer-thickness parameters for zero pressure gradient.

INTRODUCTION

Because shock-induced separation of the boundary layer is of particular interest, a number of recent analytical and experimental studies have been concerned with this phenomenon. Owing to the steep pressure gradients involved when a shock wave interacts with a turbulent boundary layer, the most promising analytic attacks on the interaction problem have been "discontinuity" analyses such as those of references 1 to 4 wherein effects of friction are considered negligible compared with effects of pressure gradient. Tyler and Shapiro (ref. 2) have assumed a power-law velocity profile ahead of the shock and a "separating" velocity profile downstream of the shock with constant pressure gradient between these stations. Crocco and Probstein (ref. 3) have applied the mixing theory of reference 5 in their analysis. Mager (ref. 4) has utilized the semi-empirical Gruschwitz auxiliary equation in conjunction with the Stewartson transformation (ref. 6) to predict the pressure rise required for shock-induced turbulent boundary-layer separation.

The present analysis is concerned with the effect of a discontinuity on a nonuniform velocity-profile characteristic of a turbulent boundary layer. In this analysis, a discontinuity is considered as an abrupt but not necessarily discontinuous change in the flow field. Although friction

is not to be considered, it is convenient to describe the discontinuity effects in terms of conventional boundary-layer-thickness parameters. The analysis utilizes a moment-of-momentum equation similar to that of reference 7, but, of course, without the shear terms. The rational nature of this moment-of-momentum equation, which retains the same form for both two-dimensional and axially symmetric flows, permits its application to a number of flow problems. For shock-induced separation, results similar to those of reference 4 are obtained and are compared with the experimental results of references 8 to 12. The effect of a discontinuity involving mass transfer (blowing or suction) upon the thickness parameters is also indicated for the case of zero pressure gradient.

ANALYSIS

The techniques of turbulent boundary-layer analysis are utilized for the present analysis. With the assumption of a constant stagnation temperature transverse to the flow surface, consideration of the rate of change of momentum in the longitudinal direction leads to an integral equation identical with the Kármán momentum integral equation except for absence of the shear terms. The corresponding moment-of-momentum equation is then obtained through multiplication of the integrand of the momentum integral equation by a distance normal to the surface Y and then integrating with respect to Y. (All symbols are defined in appendix A; appendix B outlines the development of the moment-of-momentum equation with provision for mass transfer using a form of the Stewartson transformation.)

The transformed moment-of-momentum equation with mass transfer absent takes the form

$$dH_i = -\frac{dU_e}{U_e}\frac{H_i(H_i^2 - 1)(H_i + 1)}{2} \tag{1}$$

Use of the transformed equation simplifies the analysis in that effects of Mach number need not be considered in treating the thickness parameters. Thus, H_i takes on values typical of the form-factor values encountered in incompressible-flow treatments. When the transformation relation $U_e = Ma_0$ is used, equation (1) may be written

$$\frac{dM}{M} = -\frac{2dH_i}{H_i(H_i^2 - 1)(H_i + 1)} \tag{2}$$

Upon integration, equation (2) becomes

$$AM = \frac{H_i^2}{(H_i^2 - 1)^{1/2}(H_i + 1)}\, e^{1/(H_i+1)} \equiv f(H_i) \tag{3}$$

where A is an integration constant. The right-hand side of equation (3), which will be denoted as $f(H_i)$, is plotted in figure 1. Shown for comparison in figure 1 is the equivalent of $f(H_i)$, as proposed in reference 4, which is $1/\sqrt{\eta}$ where η is the Gruschwitz form factor. The two functions differ only slightly.

For two-dimensional flow, the change in momentum thickness caused by a discontinuity is obtained by using the momentum integral equation from appendix B, again neglecting the mass-transfer term:

$$\frac{d\theta_i}{\theta_i} + (2 + H_i)\frac{dU_e}{U_e} = 0 \tag{4}$$

Using the relation $U_e = Ma_0$ and equation (2) changes equation (4) to

$$\frac{d\theta_i}{\theta_i} = \frac{2(2 + H_i)dH_i}{H_i(H_i^2 - 1)(H_i + 1)} \tag{5}$$

which upon integration yields

$$B\theta_i = \frac{(H_i^2 - 1)^{3/2}(H_i + 1)}{H_i^4} e^{-1/(H_i+1)} \equiv g(H_i) \tag{6}$$

where B is an integration constant. The right-hand side of equation (6) denoted as $g(H_i)$ is plotted in figure 2.

Thus, across a discontinuity, the Mach number ratio and momentum-thickness ratio from equations (3) and (6) are, respectively

$$\frac{M_2}{M_1} = \frac{f(H_{i,2})}{f(H_{i,1})} \tag{7}$$

$$\frac{\theta_{i,2}}{\theta_{i,1}} = \frac{g(H_{i,2})}{g(H_{i,1})} \tag{8}$$

where the subscript 1 refers to conditions ahead of the discontinuity and the subscript 2 refers to conditions behind the discontinuity. Equation (7) gives the magnitude of the discontinuity in terms of Mach number ratio necessary to change the transformed form factor from $H_{i,1}$ to $H_{i,2}$ and can also be thought of as the relation that gives the change in form factor resulting from a discontinuity of arbitrary but known magnitude. In applying equations (7) and (8) and figures 1 and 2 to compressible flow, the following relations between compressible quantities and their transformed equivalents may be useful:

$$H = H_i\left(1 + \frac{\gamma - 1}{2} M^2\right) + \frac{\gamma - 1}{2} M^2 \tag{9}$$

$$\theta = \theta_i\left(1 + \frac{\gamma - 1}{2} M^2\right)^{\frac{\gamma+1}{2(\gamma-1)}} \tag{10}$$

These relations can be obtained from the conventional definitions of the boundary-layer thickness parameters H and θ as shown in appendix C. The effect of a discontinuity on displacement thickness follows from the definition

$$H \equiv \frac{\delta^*}{\theta}$$

APPLICATIONS

Shock-Induced Separation

Equations (7) and (8) may be applied to the problem of shock-induced separation of the turbulent boundary layer if appropriate values of H_i are selected. For zero pressure gradient ahead of the shock wave a form factor $H_{i,1} = 1.286$ is assumed, which corresponds to a transformed seventh-power-law velocity profile. Such an assumption yields form factors for the physical compressible flows that are compatible with experimental observations. However, as indicated by equation (C11) of appendix C, the physical profile is not a power-law velocity profile.

Reference 13 suggests that for turbulent boundary-layer separation H_i ranges from 1.8 to 2.6. With $H_{i,2} = 2.2$, the Mach number ratio M_2/M_1 obtained from equation (7) is 0.762. As shown in figure 3, this Mach number ratio yields pressure ratios from the oblique-shock relations that are in good agreement with "first peak" pressure ratios obtained on forward-facing steps in references 8 to 11. The data of reference 12 fall below the rest; however, figure 9 of this reference suggests that these data may have been taken in the transition region. A Mach number ratio of 0.81 (obtained with $H_{i,2} = 1.72$) yields pressure ratios in good agreement with "inflection-point" pressure ratios obtained on wedges (fig. 8 of ref. 8). According to reference 8, these first-peak- and inflection-point pressure ratios provide first approximations to the pressure ratios for which separation is likely to be encountered on control-surface configurations.

The pressure ratios obtained from the oblique-shock relations and equation (4) of reference 4 which states, in the notation of this paper, that $\frac{M_2}{M_1} = \sqrt{0.494} = 0.703$ are presented in figure 3 as are also the pressure ratios obtained from equation (8) of reference 4. Inasmuch as

the results from equations (4) and (8) of reference 4 should be in agreement, the discrepancy shown in figure 3 suggests that the oblique-shock linearization used in equation (8) of reference 4 is inadequate. The result of reference 4 overestimates the pressure ratios obtained experimentally on forward-facing steps.

Effects of pressure gradient. - The present analysis can be applied to the case of favorable or adverse pressure gradient ahead of the shock when the appropriate form factors are known. Qualitatively it is known that the form factors for adverse and favorable pressure gradients are, respectively, greater and less than the flat-plate form factor. Thus, for favorable pressure gradients ahead of the shock, a stronger shock is required, whereas for adverse pressure gradients ahead of the shock, a weaker shock would separate the turbulent boundary layer.

For the case of boundary-layer development under an adverse pressure gradient large relative to the skin-friction term but where the incident shock is of insufficient strength to separate the flow, equations (7) to (10) may be used to obtain the change in H_i, θ_i, and δ_i^* across the shock. The remaining development to separation requires solution of the equations of the compressible turbulent boundary layer with a stipulated skin-friction relation.

Effect of Mass Transfer

The effect of suction or blowing on form factor for two-dimensional flat-plate flow may be approximately evaluated by using the momentum integral and moment-of-momentum equations of appendix B. The method requires that the skin-friction coefficient be negligible relative to the mass-transfer coefficient $\frac{\rho_w v_w}{\rho_e u_e}$. In the vicinity of the mass-transfer region, the pressure gradient terms may be appreciable. The following analysis, which omits consideration of pressure gradient, may thus yield only qualitative results. A similar analysis for flow over a cone is given in appendix D. For two-dimensional flow, the momentum integral and moment-of-momentum equations are, respectively,

$$\frac{d\theta_i}{dX} - \frac{V_w}{U_e} = 0 \tag{11}$$

and

$$\theta_i \frac{dH_i}{dX} = (H_i^2 - 1) \frac{V_w}{U_e} \tag{12}$$

Eliminating the quantity V_w/U_e between equations (11) and (12) yields

$$\frac{dH_i}{H_i^2 - 1} = \frac{d\theta_i}{\theta_i}$$

which upon integration becomes

$$C\theta_i = \sqrt{\frac{H_i - 1}{H_i + 1}} \equiv R(H_i) \tag{13}$$

where C is an integration constant, or

$$\frac{\theta_{i,2}}{\theta_{i,1}} = \frac{R(H_{i,2})}{R(H_{i,1})} \tag{14}$$

where the subscripts 1 and 2 refer, respectively, to conditions before and after the mass transfer. The function $R(H_i)$ is plotted in figure 4.

The relation between the transformed momentum-thickness ratio and the mass transfer is obtained from the momentum equation with the assumption that V_w/U_e is constant for the region of mass transfer. Thus upon integration, equation (11) becomes

$$\theta_{i,2} = \frac{\rho_w v_w x}{\rho_0 a_0 M} + \theta_{i,1}$$

or, since $m = \rho_w v_w x$, represents the mass flow per unit width

$$\frac{\theta_{i,2}}{\theta_{i,1}} = 1 + \frac{m}{\rho_0 a_0 M \theta_{i,1}} \tag{15}$$

Expressing the mass transfer as a fraction of the boundary-layer mass flow ahead of the transfer region transforms equation (15) into

$$\frac{\theta_{i,2}}{\theta_{i,1}} = 1 + \mu\left(\frac{\delta_1}{\theta_1} - H_1\right) \tag{16}$$

where the mass-transfer coefficient μ is defined as

$$\mu \equiv \frac{m}{\rho_e u_e (\delta_1 - \delta_1^*)} \tag{17}$$

The quantities θ_1/δ_1 and H_1 are tabulated for certain typical power-law profiles in reference 14.

The amount of mass removal by suction ahead of a normal shock that is required to prevent flow separation behind the shock may be estimated in the absence of pressure gradient ahead of the shock and for negligible skin friction. The form factor ahead of the normal shock for incipient separation is found from equation (7) and the mass removal required to obtain this form factor is determined from equations (14) and (16). For an assumed seventh-power-law transformed-velocity profile and with $H_{i,2} = 2.2$, the percentage of boundary-layer mass flow to be removed rises steeply with Mach number, reaches a peak of about 8 percent at $M \approx 3$, and gradually decreases at higher Mach numbers. The mass flow to be removed, however, will increase with Mach number for constant ambient pressure and temperature. In the absence of experimental data, these results must be considered qualitative. The method cannot be used to estimate the effects of mass transfer behind shock-induced separation, since the analysis does not apply after the onset of separation.

SUMMARY OF RESULTS

A method has been devised for calculating the change of boundary-layer-thickness parameters and form factor caused by a discontinuity in the absence of friction effects. The form of the result suggests that the Mach number ratio across the shock is a characteristic parameter for defining shock-induced separation. The experimental data for forward-facing steps and for wedges are well described by the curves of constant Mach number ratio (ratio of Mach number ahead of to that behind discontinuity) $M_2/M_1 \approx 0.76$ and $M_2/M_1 \approx 0.81$, respectively. The method has also been applied to estimate the amount of mass removal that is required ahead of a normal shock to prevent flow separation behind the shock.

Lewis Flight Propulsion Laboratory
National Advisory Committee for Aeronautics
Cleveland, Ohio, April 11, 1955

APPENDIX A

SYMBOLS

The following symbols are used in this report:

A, B, C	integration constants
a	velocity of sound
$f(H_i)$	$\equiv \dfrac{H_i^2 \, e^{1/(H_i+1)}}{(H_i^2 - 1)^{1/2} \, (H_i + 1)}$
$g(H_i)$	$\equiv \dfrac{(H_i^2 - 1)^{3/2} \, (H_i + 1)}{H_i^4} \, e^{-1/(H_i+1)}$
H	form factor, $H \equiv \delta^*/\theta$
M	free-stream Mach number
m	mass transfer per unit width
N	power-law velocity profile parameter, $\dfrac{u}{u_e} = \left(\dfrac{y}{\delta}\right)^{1/N}$
p	pressure
r	radius of axially symmetric body
$R(H_i)$	$\equiv \sqrt{\dfrac{H_i - 1}{H_i + 1}}$
t	temperature
U	transformed longitudinal velocity
u	longitudinal velocity
V	transformed normal velocity
v	normal velocity
X	transformed longitudinal coordinate

x	longitudinal coordinate
Y	transformed normal coordinate
y	normal coordinate
γ	ratio of specific heats
δ	boundary-layer thickness
δ^*	displacement thickness
δ_i^*	transformed displacement thickness, $\int_0^{\delta_i}\left(1 - \frac{U}{U_e}\right) dY$
η	Gruschwitz form factor, $1 - \left[\frac{H_i - 1}{H_i(H_i + 1)}\right]^{H_i - 1}$
μ	mass-transfer coefficient
θ	momentum thickness
θ_i	transformed momentum thickness, $\int_0^{\delta_i} \frac{U}{U_e}\left(1 - \frac{U}{U_e}\right) dY$
ρ	density
τ	shear stress

Subscripts:

e	free stream ("external")
i	transformed or "incompressible" value
s	stagnation value
w	wall value
0	free-stream stagnation value ahead of discontinuity
1	conditions ahead of discontinuity
2	conditions behind discontinuity

APPENDIX B

DEVELOPMENT OF MOMENT-OF-MOMENTUM EQUATION

The behavior of nonuniform profiles of the boundary-layer type in a compressible flow can be studied from continuity and momentum considerations. In examining this behavior, the effects of shear are neglected, although presumably the nonuniform profiles might have been set up through shearing action. With the stagnation temperature in the transverse direction considered to be constant, the equations of motion are

Continuity:

$$\frac{\partial}{\partial x}(\rho u) + \frac{\partial}{\partial y}(\rho v) = 0$$

Momentum:

$$\rho u \frac{\partial u}{\partial x} + \rho v \frac{\partial u}{\partial y} = -\frac{\partial p}{\partial x} \qquad \text{(B1)}$$

Equations (B1) resemble the boundary-layer equations except that the friction term is lacking from the momentum equation. The application of a Stewartson transformation to equations (B1) and reduction of the result to an integral equation follow the procedure of reference 15. A modified Stewartson transformation can be described by the following coordinate transformations:

$$dX = \frac{p_e}{p_0}\frac{a_e}{a_0}\,dx$$

$$dY = \frac{\rho}{\rho_0}\frac{a_e}{a_0}\,dy \qquad \text{(B2)}$$

The transformed coordinates are now represented by upper-case letters (X, Y) and the subscript e refers to local conditions at the outer edge of the boundary-layer-type profile. The subscript 0 denotes reference values, which are here taken as free-stream stagnation values ahead of the discontinuity. The relation between transformed and physical longitudinal velocities resulting from the Stewartson transformation is

$U = \frac{a_0}{a_e} u$ or for the external flow, $U_e = Ma_0$.

From the method of reference 15, the integrand of the momentum integral equation is formed. The result for the case of the present paper is

$$[U(U_e - U)]_X + [V(U_e - U)]_Y + U_{e_X}(U_e - U) = 0 \qquad \text{(B3)}$$

When equation (B3) is integrated with respect to Y between Y = 0 and Y = δ_i, where δ_i is the transformed boundary-layer thickness, the transformed momentum integral equation is obtained:

$$\frac{d\theta_i}{dX} + \frac{\theta_i(2 + H_i)}{U_e}\frac{dU_e}{dX} - \frac{V_w}{U_e} = 0 \qquad \text{(B4)}$$

where V_w/U_e is the term representing the effect of mass transfer.

If the integrand (B3) is multiplied by Y and the resulting relation integrated with respect to Y, the moment-of-momentum relation is obtained as indicated, for example, in reference 7. The moment-of-momentum equation in the transformed plane can be written

$$\theta_i \frac{dH_i}{dX} = -\frac{\theta_i}{U_e}\frac{dU_e}{dX}\frac{H_i(H_i^2 - 1)(H_i + 1)}{2} + (H_i^2 - 1)\frac{V_w}{U_e} \qquad \text{(B5)}$$

Application of equations (B4) and (B5) to turbulent flow implies that densities and velocities are time-averaged quantities and that the correlation terms (those involving products of perturbation quantities) are negligible.

APPENDIX C

RELATION OF COMPRESSIBLE AND TRANSFORMED BOUNDARY-LAYER FORM FACTORS

The relation between compressible and transformed boundary-layer form factors will be formulated through the individual relations for momentum and displacement thicknesses, respectively. Although the procedures of the present paper are for flows with constant stagnation temperature in the transverse direction, the results of this appendix apply also to the case of variable stagnation temperature in the transverse direction.

Momentum Thickness

The momentum thickness of a compressible boundary layer is defined as

$$\theta = \int_0^{\delta} \frac{\rho u}{\rho_e u_e}\left(1 - \frac{u}{u_e}\right) dy \tag{C1}$$

Using relations (B4) and the knowledge that $\frac{U}{U_e} = \frac{u}{u_e}$ changes equation (C1) to

$$\theta = \theta_i \left(\frac{p_0}{p_e}\frac{a_e}{a_0}\right) \tag{C2}$$

where

$$\theta_i = \int_0^{\delta_i} \frac{U}{U_e}\left(1 - \frac{U}{U_e}\right) dY \tag{C3}$$

Displacement Thickness

The displacement thickness of a compressible boundary layer is defined as

$$\delta^* = \int_0^{\delta} \left(1 - \frac{\rho u}{\rho_e u_e}\right) dy \tag{C4}$$

With constant pressure through the boundary layer, equation (C4) can be rewritten as

$$\delta^* = \int_0^{\delta} \frac{t_e}{t}\left(\frac{t}{t_e} - \frac{u}{u_e}\right) dy \tag{C5}$$

The static-temperature distribution in the boundary layer can be written

$$\frac{t}{t_e} = \frac{t_s}{t_0}\left(1 + \frac{\gamma - 1}{2} M^2\right) - \frac{\gamma - 1}{2} M^2 \left(\frac{u}{u_e}\right)^2 \tag{C6}$$

where t_s is the stagnation temperature corresponding to the static temperature t.

Then

$$\delta^* = \int_0^{\delta_i} \frac{t_e}{t}\left[\frac{t_s}{t_0} + \frac{\gamma - 1}{2} M^2 \left(\frac{t_s}{t_0} - \frac{U^2}{U_e^2}\right) - \frac{U}{U_e}\right]\frac{\rho_0 a_0}{\rho a_e} dY$$

$$= \left(\frac{p_0}{p_e}\right)\left(\frac{a_e}{a_0}\right)\left[\delta_i^* + \frac{\gamma - 1}{2} M^2 \left(\delta_i^* + \theta_i\right)\right] \tag{C7}$$

where

$$\delta_i^* = \int_0^{\delta_i}\left[\left(\frac{t_s}{t_0} - 1\right) + \left(1 - \frac{U}{U_e}\right)\right] dY = \int_0^{\delta_i}\left(\frac{t_s}{t_0} - \frac{U}{U_e}\right) dY \tag{C8}$$

which for constant stagnation temperature through the boundary layer is

$$\delta_i^* = \int_0^{\delta_i}\left(1 - \frac{U}{U_e}\right) dY \tag{C9}$$

Since $H = \delta^*/\theta$ and $H_i = \delta_i^*/\theta_i$, equations (C2) and (C7) with the definitions (C3) and (C8) yield

$$H = H_i + \frac{\gamma - 1}{2} M^2 \left(H_i + 1\right) \tag{C10}$$

or

$$H = H_i\left(1 + \frac{\gamma - 1}{2} M^2\right) + \frac{\gamma - 1}{2} M^2 \tag{6}$$

The Stewartson transformation causes distortion of the velocity profile with increasing Mach number M. Assume that the transformed- and physical-velocity profiles are the power-law profiles $\frac{u}{u_e} = \left(\frac{y}{\delta}\right)^{1/N}$ and $\frac{U}{U_e} = \left(\frac{Y}{\delta_i}\right)^{1/N_i}$. With $\frac{u}{u_e} = \frac{U}{U_e}$ and $\delta = \int_0^{\delta_i} \frac{\rho_0 a_0}{\rho a_e} dY$, the transformation leads to the relation for $\gamma = 1.4$

$$\left(\frac{U}{U_e}\right)^{N-N_i} = \frac{5 + M^2 - \frac{M^2 N_i}{2 + N_i}\left(\frac{U}{U_e}\right)^2}{5 + M^2 - \frac{M^2 N_i}{2 + N_i}} \qquad \text{(C11)}$$

Equation (C11) indicates that if N_i is taken to be constant as in a standard power-law velocity profile, then the physical profile parameter N will vary with the normal coordinate y. This variation is accentuated with increasing Mach number.

APPENDIX D

DERIVATION OF RELATIONS FOR AXIALLY SYMMETRIC FLOW

For axially symmetric flow, the equations corresponding to (B4) and (B5) are

Momentum:

$$\frac{d\theta_i}{dX} + \frac{\theta_i(2 + H_i)}{U_e}\frac{dU_e}{dX} + \frac{\theta_i}{r}\frac{dr}{dX} - \frac{V_w}{U_e} = 0 \tag{D1}$$

Moment of Momentum:

$$\theta_i \frac{dH_i}{dX} = (H_i^2 - 1)\frac{V_w}{U_e} - \frac{\theta_i}{U_e}\frac{dU_e}{dX}\frac{H_i(H_i^2 - 1)(H_i + 1)}{2} \tag{D2}$$

The moment-of-momentum equation is the same for axially symmetric as for two-dimensional flow. Thus,

$$\frac{M_2}{M_1} = \frac{f(H_{i,2})}{f(H_{i,1})} \tag{7}$$

is correct for axially symmetric flow. Examination of the momentum integral equation (D1) shows that the axially symmetric equivalent of equation (8) is written

$$\frac{(r\theta_i)_2}{(r\theta_i)_1} = \frac{g(H_{i,2})}{g(H_{i,1})} \tag{D3}$$

Since across a discontinuity, the radii $r_1 = r_2$, equation (D3) is essentially that for two-dimensional flow.

Consideration of suction or blowing on a cone in a manner analogous to that for two-dimensional flat-plate flow leads to the following equations as equivalents for equations (14), (15), and (16), respectively:

$$\frac{(r\theta_i)_2}{(r\theta_i)_1} = \frac{R(H_{i,2})}{R(H_{i,1})} \tag{D4}$$

$$\frac{(r\theta_i)_2}{(r\theta_i)_1} = 1 + \frac{m}{2\pi\rho_0 a_0 M(r\theta_i)_1} \tag{D5}$$

$$\frac{(r\theta_i)_2}{(r\theta_i)_1} = 1 + \mu\left(\frac{\delta_1}{\theta_1} - H_1\right) \tag{D6}$$

where m now represents the total mass transfer and μ, which is still the ratio of mass transferred to the boundary-layer mass flow, is now defined

$$\mu \equiv \frac{m}{2\pi r_1 \rho_e u_e (\delta_1 - \delta_1^*)} \tag{D7}$$

REFERENCES

1. Nitzberg, Gerald E., and Crandall, Stewart: Some Fundamental Similarities Between Boundary-Layer Flow at Transonic and Low Speeds. NACA TN 1623, 1948.

2. Tyler, Robert D., and Shapiro, Ascher H.: Pressure Rise Required for Separation in Interaction Between Turbulent Boundary Layer and Shock Wave. Jour. Aero. Sci., vol. 20, no. 12, Dec. 1953, pp. 858-860.

3. Crocco, Luigi, and Probstein, Ronald F.: The Peak Pressure Rise Across an Oblique Shock Emerging from a Turbulent Boundary Layer Over a Plane Surface. Rep. No. 254, Dept. Aero. Eng., Princeton Univ., Mar. 1954. (Contract N60onr-270, Task Order 6, Proj. No. NR-061-049.)

4. Mager, Artur: Prediction of Shock-Induced Turbulent Boundary-Layer Separation. Jour. Aero. Sci., vol. 22, no. 3, Mar. 1955, pp. 201-202.

5. Crocco, Luigi, and Lees, Lester: A Mixing Theory of the Interaction Between Dissipative Flows and Nearly Isentropic Streams. Jour. Aero. Sci., vol. 19, no. 10, Oct. 1952, pp. 649-676.

6. Stewartson, K.: Correlated Incompressible and Compressible Boundary Layers. Proc. Roy. Soc. (London), ser. A, vol. 200, no. A1060, Dec. 22, 1949, pp. 84-100.

7. Tetervin, Neal, and Lin, Chia Chiao: A General Integral Form of the Boundary-Layer Equation for Incompressible Flow with an Application to the Calculation of the Separation Point of Turbulent Boundary Layers. NACA Rep. 1046, 1951. (Supersedes NACA TN 2158.)

8. Lange, Roy H.: Present Status of Information Relative to the Prediction of Shock-Induced Boundary-Layer Separation. NACA TN 3065, 1954.

9. Bogdonoff, S. M., and Kepler, C. E.: Separation of a Supersonic Turbulent Boundary Layer. Rep. No. 249, Dept. Aero. Eng., Princeton Univ., Jan. 1954. (Contract No. N6-onr-270, Task Order 6, Proj. No. NR-061-049.)

10. Bernstein, Harry, and Brunk, William E.: Exploratory Investigation at $M = 2$ of the Flow in the Separated Region Ahead of Two Blunt Bodies. NACA RM E55D07b, 1955.

11. Love, Eugene S.: On the Effect of Reynolds Number upon the Peak Pressure Rise Coefficient Associated with Separation of a Turbulent Boundary Layer in Supersonic Flow. Jour. Aero. Sci., vol. 22, no. 5, May 1955.

12. Barry, F. W.: A Review of Experimental Results on Boundary Layer - Shock Wave Interaction. Rep. No. AL-1599, North American Aviation, Inc., Dec. 15, 1952. (Proj. MX-770.)

13. von Doenhoff, Albert E., and Tetervin, Neal: Determination of General Relations for the Behavior of Turbulent Boundary Layers. NACA Rep. 772, 1943. (Supersedes NACA WR L-382.)

14. Tucker, Maurice: Approximate Calculations of Turbulent Boundary-Layer Development in Compressible Flow. NACA TN 2337, 1951.

15. Cohen, Clarence B., and Reshotko, Eli: The Compressible Laminar Boundary Layer with Heat Transfer and Arbitrary Pressure Gradient. NACA TN 3326, 1955.

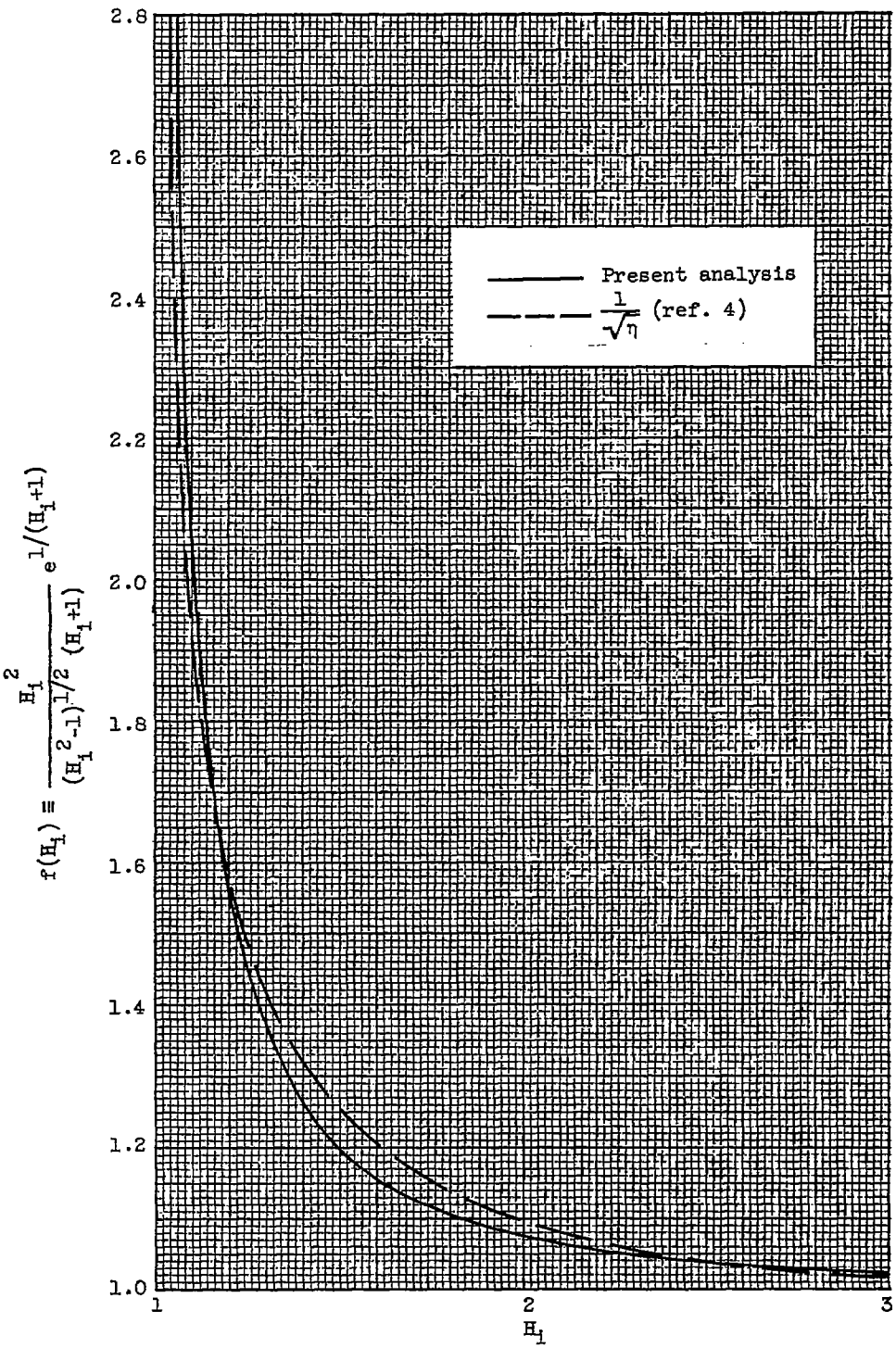

Figure 1. - Function for determining Mach number ratio.

$$\frac{M_2}{M_1} = \frac{f(H_{1,2})}{f(H_{1,1})}$$

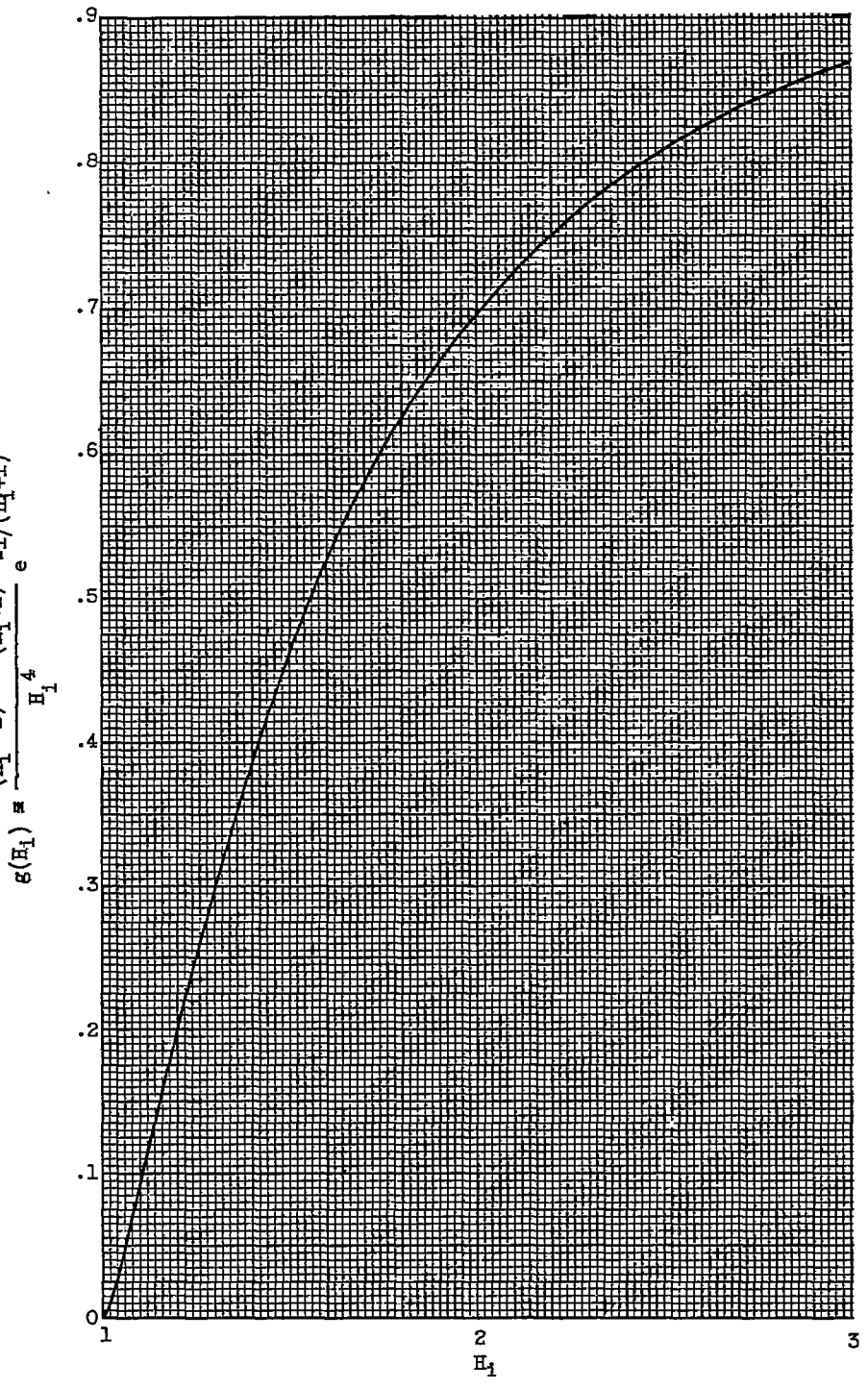

Figure 2. - Function for determining momentum-thickness ratio.

$$\frac{\theta_{i,2}}{\theta_{i,1}} = \frac{g(H_{i,2})}{g(H_{i,1})}$$

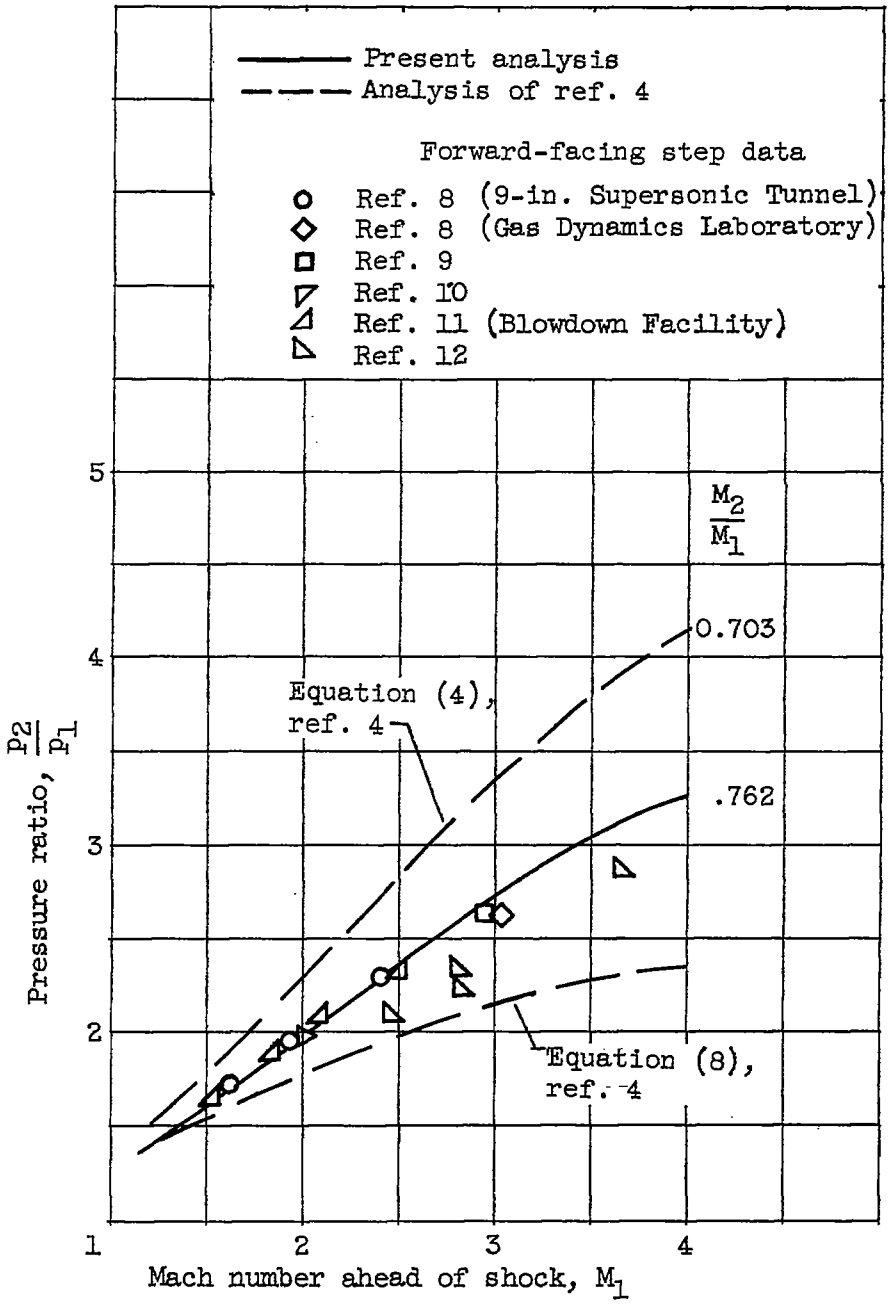

Figure 3. - Pressure ratio for shock-induced, turbulent, boundary-layer separation.

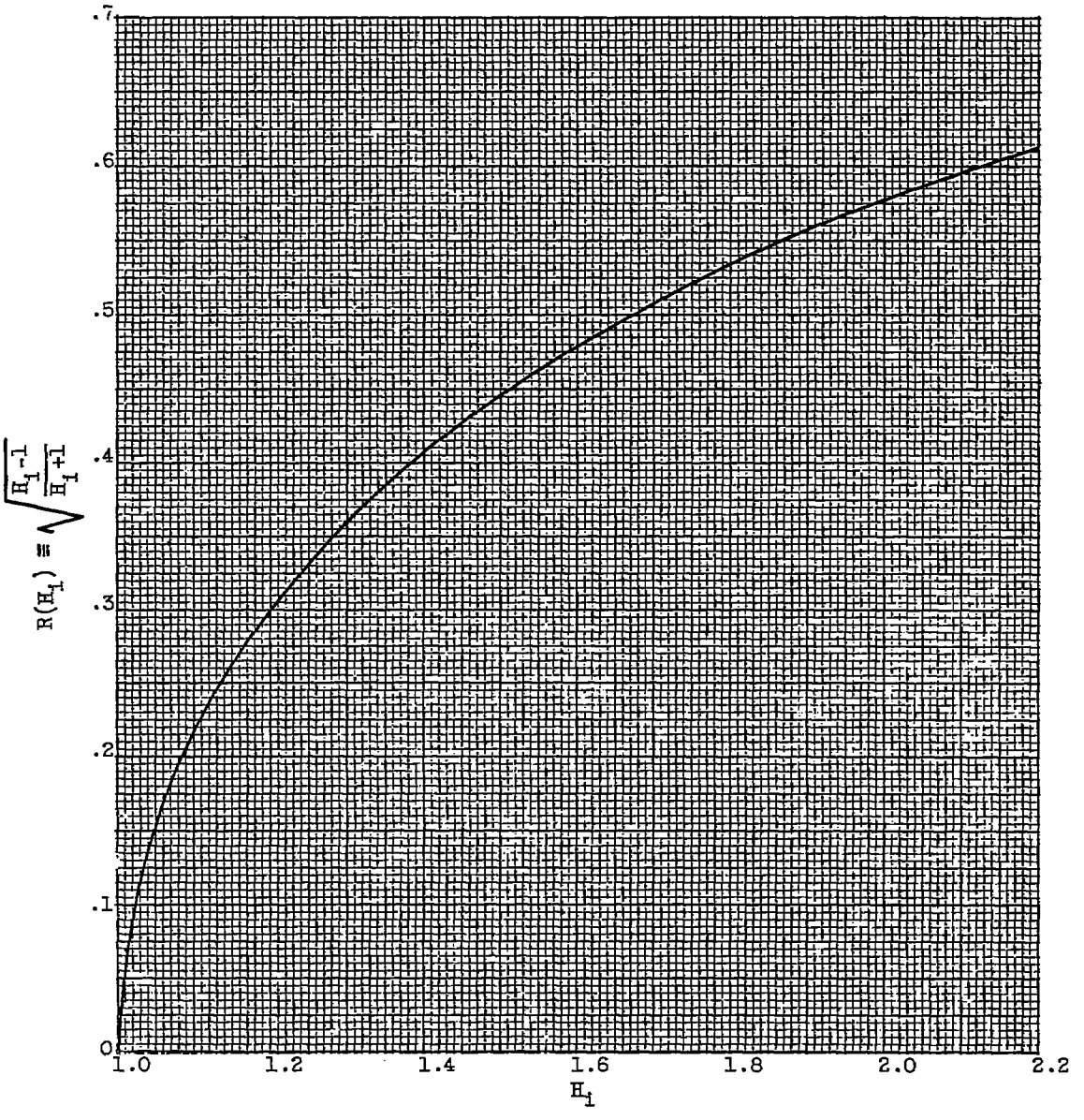

Figure 4. - Function for determining effects of mass transfer on transformed momentum-thickness ratio.

$$\frac{\theta_{i,2}}{\theta_{i,1}} = \frac{R(H_{i,2})}{R(H_{i,1})}$$